# Visualization by freeze fracture, in vitro and in vivo, of the products of fat digestion

**M. W. Rigler, R. E. Honkanen, and J. S. Patton**[1]

Department of Microbiology, The University of Georgia, Athens, GA 30602

**Abstract** The technique of freeze fracture was used to visualize triglyceride (TG) hydrolysis and the production of lipolytic products (LPs) in vitro and in vivo in the presence of bile salts (BS). Three systems were investigated: *1*) pure lipolytic products (oleic acid and monoolein) in the presence of a pure bile salt (taurodeoxycholate (TDC)), *2*) lipolytic products produced from TG by pancreatic lipase in the presence of a variety of bile salts, and *3*) lipolytic products produced in the intestine of the killifish, *Fundulus heteroclitus,* after fat feeding. In vitro, lamellae (4–5 nm thick with 0–8-nm water spacings) appeared on the surface of TG droplets in all preparations with LP/BS molar ratios of 1.5 or greater and spherical vesicles (diameter range, 20–130 nm) were produced from these lamellae. With model killifish bile (taurocholate–cholate 1:1) at LP/BS ratios between 1.5 and 4, homogeneous vesicles or particles (mean diameter, 23.8 nm) were produced by lipase at pH 6.9. In vivo, lamellar product phases also occurred after fat feeding. The smallest visible LP/BS structures by freeze fracture electron microscopy were ~20 nm globular particles. Large disc-shaped micelles either were not present or were below the resolution limit of the replica (~10 nm). The dominant aggregated lipolytic product phase was composed of multiple layers of rough-textured lamellae. No evidence of cubic structure was seen. These results show that lamellar and vesicular lipolytic product phases can be intermediates in intestinal fat digestion. However, no evidence for the direct endocytotic absorption of these product phases by the intestinal microvillus membrane was found.—**Rigler, M. W., R. E. Honkanen, and J. S. Patton.** Visualization by freeze fracture, in vitro and in vivo, of the products of fat digestion. *J. Lipid Res.* 1986. **27:** 836–857.

**Supplementary key words** lipid digestion • fat absorption • intestinal • bile salts • lipid phases

Following centrifugation, intestinal contents have been operationally defined by Hofmann and Borgström (1, 2) as containing two phases during the digestion of a fat meal: an oil phase containing triglyceride, diglyceride, monoglyceride, and free fatty acids, and a micellar phase containing primarily bile salts, free fatty acids, and monoglycerides. A true micellar solution should be optically clear and free of large light-scattering particles (Tyndall effect). However, Hofmann and Borgström (2) sometimes described the micellar phase as "opalescent," "turbid," and containing 3- to 10-micron-sized particles (2). In optically clear micellar systems containing taurodeoxycholate and lipolytic products (monoolein and oleic acid = LPs), Hofmann and Borgström showed that the addition of excess LP produced an opalescent solution. Opalescence was attributed to micelle splitting, micelle size increase, and/or liquid crystalline production. By light microscopy, Patton and Carey (3) have shown that crystalline and liquid crystalline product phases are produced from triglyceride emulsions in the presence of lipase, colipase, and bile salts and, recently, freeze fracture electron microscopy has revealed that, at pH 8.3, similar preparations produce liquid crystalline phases in the absence of bile salts (4). Laser light-scattering studies in systems containing cholesterol, phospholipids, and bile salts (5), or monoglycerides, free fatty acids, and bile salts (6, 7) suggest that bile salts and lipids can form disc-shaped micelles, liquid crystalline "microprecipitates," and vesicles depending on the lipid/bile salt ratio. Using NMR spectroscopy, Müller (8) has also demonstrated micelles and vesicles in analogous systems. Mazur, Benedek, and Carey (9) have suggested that vesicles and large mixed micelles coexist at the micelle phase boundary in systems containing lecithin and bile salts. From these observations it now appears that the oil–micellar view of fat digestion has been an oversimplification and that other phases may occur during the hydrolysis of triglyceride under physiological conditions.

Abbreviations: TG, triglyceride; LPs, lipolytic products; TEM, transmission electron microscopy; BS, bile salts; TLC, thin-layer chromatography; TB, tributyrin; PMSF, phenylmethylsulfonyl fluoride; MG, monoacylglycerol; TDC, taurodeoxycholate; TC, taurocholate; CMC, critical micellar concentration; VLDL, very low density lipoproteins.

[1]Address reprint requests to: John S. Patton, Pharmacology Department, Genentech, Inc., South San Francisco, CA 94080.

The primary goal of this study was to examine fat digestion by pancreatic lipase in the presence of bile salts at the ultrastructural level. In the past, transmission electron microscopy (TEM) was utilized as a tool to study fat digestion and micelle morphology (10–19). However, TEM has many drawbacks such as: *a*) the production of artifacts caused by fixation techniques, *b*) the inability to precisely halt the process of lipolysis and, most importantly, *c*) the solubilization and extraction of lipid by chemical dehydrants and embedments (20, 21). To circumvent these problems we chose to visualize the events of fat digestion and absorption in vivo with the technique of freeze fracture. It is the best ultrastructural method available for preserving water-dependent lipid phases because no dehydration steps are involved in specimen preparation. Using a jet of liquified propane (−160°C), intestinal tissue and luminal contents can be fixed almost instantaneously, and lipid phase transitions are minimized due to the extremely high cooling velocity (~10,000 °K/sec) (22).

In this study the freeze fracture ultrastructure of fat digestion was examined in a variety of systems to better understand the effects of bile salts on lipolytic product morphology in vitro and in vivo. In vitro, model systems containing pure lipolytic products and bile salts over a wide range of LP/BS ratios were investigated. In addition, systems containing physiological concentrations of lipase, triglyceride, and bile salts were examined. In vivo lipolysis was followed after feeding fat to the carnivorous salt marsh killifish (*Fundulus heteroclitus*). The hardy killifish was chosen for several reasons. The small diameter of its simple intestine (~3–5 mm) allows for rapid removal and freezing with the contents intact. Since it is maintained at room temperature, its intestine can be removed and placed in the rapid freezing device without an additional temperature drop. In addition, fat assimilation in teleosts resembles that of mammals (23–26) and killifish bile contains only two major bile acids and little or no phospholipid. Therefore, lipolytic products generated in vivo could be compared to those produced in vitro.

## MATERIALS AND METHODS

### Materials

The following materials were obtained from Sigma Chemical Co. (St. Louis, MO): phenylmethylsulfonyl fluoride (PSMF), sodium azide, gum arabic, olive oil, trioleoylglycerol, tributyrylglycerol; and oleic acid. All oils were found to be 99% pure or better by thin-layer chromatography (TLC). The sodium salts of taurodeoxycholate (TDC), taurocholate (TC), cholate, (99% pure from Calbiochem-Behringer, La Jolla, CA) were used without further purification. Casamino acids (vitamin assay grade) were obtained from Difco Laboratories, Detroit, MI, and powdered porcine pancreatic lipase (triacylglycerol hydrolase, E.C. 3.1.1.3) was from Calbiochem-Behringer. Pure porcine pro-colipase/colipase powder was a gift from Bengt Borgström and Mats Lindström of the University of Lund, Sweden. Pig bile and pancreatic juice were collected fresh as described below. [$^{14}$C]Trioleoylglycerol (180 mCi/mmol, radiopurity 99% by TLC) was purchased from RoseChem Products, Los Angeles, CA and [$^{3}$H]taurocholate (6.6 Ci/mmol, radiopurity 99% by TLC) was from New England Nuclear, Boston, MA. All solvents were of pesticide grade quality or better.

### Pure lipase, colipase, and monoglyceride purification

Porcine pancreatic powder was delipidated by the method of Verger et al. (27) and pancreatic lipase was purified according to a modified method of Rovery, Boudouard, and Bianchietta (28) by replacing the DE-11 with DE-23 and omitting the final CM-cellulose step which separates lipase isozymes. Samples of enzyme were stored at −20°C in a buffer containing 5 mM Tris HCl, 3.3 mM $CaCl_2$, 18.2 mM NaCl, and 1 mM benzamidine at pH 8.0. Lipase activity was measured potentiometrically at pH 8.0 and 23°C in an assay containing 0.5 ml of tributyrin (TB) and 10 ml of buffer containing 2 mM Tris maleate, 150 mM NaCl, 1 mM $CaCl_2$, and 0.02% $NaN_3$, pH 8.3 (1 TB unit = 1 μmol of tributyrate produced per min per ml). The final activity was 3620 TB units/ml. Radiolabeled substrate was made by adding 60 μl of [$^{14}$C]triolein in hexane (28 nmol, sp act 105.6 mCi/mmol) to 50 μl of olive oil and bubbling the mixture with $N_2$ until the hexane was removed (3–4 hr at 37°C).

Porcine pro-colipase I (101 residues) was purified by Mats Lindström as previously described (29). The final activity was 91 TB units/ml when 10 μg of colipase and 20 μg of lipase were combined in 10 ml of buffer, at pH 8.0. Typically, 40 μl of purified lipase (650 TB units/ml) was combined with 2 μl of pro-colipase (2 mg of pro-colipase dissolved in 40 μl of a buffer containing 5 mM Tris-HCl, 3.3 $CaCl_2$, 18.2 mM NaCl, and 1 mM benzamidine at pH 8.0) prior to an experiment.

Crude lipase preparations were used to make monoglycerides as follows. Delipidated pancreatic lipase powder (0.2 mg) was stirred for 20 min in 5 ml of buffer containing 100 mM Tris base, 0.5 mM PMSF, 1 mM benzamidine, and 0.02% $NaN_3$ at pH 9.0. The mixture was centrifuged at 15,000 *g* for 4 min and the supernatant (2500 TB units per min per ml) was used without further purification. An emulsion of olive oil was prepared by agitating, for 3 min at top speed with a Vortex-Genie (Fisher Scientific, Atlanta, GA), a mixture of 10% gum arabic in 2 mM Tris base buffer (pH 8.5) containing 150 mM NaCl and 1 mM $CaCl_2$ in a 2:1 ratio (v/v) with the oil. One ml of the olive oil emulsion was added to 4 ml of the lipase preparation and the reaction was titrated at room temperature with 0.05 N NaOH at pH 8.5 on a TTT pH stat

(Radiometer, Copenhagen, Denmark). After 20 min, the reaction was stopped by acidifying the mixture to pH 1.7 with 5 N HCl. Lipids were extracted with five volumes of diethyl ether and centrifuged at 2000 *g* for 2–5 min. The ether extract was back-extracted against $H_2O$ (to remove excess buffer salt) and then evaporated under a stream of $N_2$. Reaction products were dissolved in 1 ml of $CHCl_3$–MeOH 1:1 and 200 μl was spotted on a 20 × 20 cm Silica Gel 60 TLC plate (Bodman Chemical Co., Doraville, GA) and separated using a diethyl ether–$NH_4OH$ 100:1 solvent system. The entire MG band was scraped off and eluted with 7 ml of diethyl ether. The ether was evaporated with $N_2$ and the amount of MG was quantified gravimetrically. MGs were stored in $CHCl_3$–MeOH 1:1 at 4°C under $N_2$ until needed.

### Pig bile and pancreatic juice collection

The common bile duct and the pancreatic duct of a 50-kg pig were cannulated. Bile and pancreatic juice were collected over a period of 3 days. The activity of the pancreatic juice was measured using tributyrin as substrate and found to be 4000 units/ml. Pancreatic juice was used without further purification. Bile was stored at −20°C prior to use, then thawed and centrifuged (2120 *g* as above) and the overlying lipid layer was removed by aspiration. The total concentration of bile salts in porcine bile was quantified on Chromarods as previously described (30).

### Lipolytic products in pure bile salt

Pure lipolytic products (LPs) (MGs and oleic acid 3:1 (w/w)) at 64, 32, and 16 mM were combined in a buffer containing 8 mM NaTDC, 150 mM NaCl, 50 mM Tris base, and 30% glycerol at pH 6.5. Lipolytic product concentrations of 32 and 16 mM were obtained by serial dilution of the 64-mM preparation. All of these control mixtures were stirred at 23°C in the dark for 1–2 hr. Samples were then processed for freeze fracture.

### Lipase reactions in the presence of bile salts

Three reaction mixtures utilizing combinations of bile salts and lipases were examined. The first mixture contained 650 TB units lipase–colipase/ml and 4 mM bile salts. Lipase buffer 1, (195 μl) was combined with 15 μl of substrate, 60 μl of a bile salt solution, and 30 μl of purified lipase/colipase preparation. Lipase buffer 1 consisted of 150 mM NaCl, 100 mM Tris maleate, 0.1 mM $CaCl_2$, 10% glycerol, and 0.02% $NaN_3$ at pH 6.95. Substrate consisted of an emulsion made from olive oil by sonicating (60 W for 10–20 sec) 1 ml of oil in 2 ml of a 10% gum arabic solution in lipase buffer 1. Prior to dilution in the reaction mixture, the bile salt solution consisted of 20 mM pure cholate–taurocholate 1:1 (w/w) in lipase buffer 1 at pH 6.95. The reaction was run at 23°C and the pH was monitored during constant stirring with an MI 410 microcombination pH probe (tip diameter 1.2 mm) (Microelectrodes, Inc., Londonderry, NH). Samples (2 μl) were remove at 0, 1, 2.5, 5, 10, 20, and 30 min intervals from stirred and nonstirred mixtures, then processed for freeze fracture. To determine the total lipolytic product concentration, samples (20 μl) were removed from the reaction mixture, extracted in diethyl ether, dried with $N_2$, and redissolved in $CHCl_3$–MeOH 1:1. Samples were then spotted on TLC plates, run to 1 cm above the origin in acetone, then run to 10 cm above the origin in a diethyl ether–$NH_4OH$ 100:1 system. In this way bile salts remained at the origin and radiolabeled products were separated.

The second mixture contained 1380 TB units per min per ml of pancreatic juice and 42 mM porcine bile salts. Porcine pancreatic juice (20 μl) was combine with 10 μl of porcine bile, 18 μl of glycerol, and 10 μl of substrate. The substrate was prepared as described above, except the buffer contained 150 mM NaCl, 40 mM Tris–HCl, 1 mM $CaCl_2$, and 0.02% $NaN_3$ (termed "lipase buffer 2") at pH 7.00. This reaction mixture was incubated at 23°C for 1–2 hr prior to freeze fracture.

The third mixture contained 1500 TB units lipase–colipase/ml and 17.2 mM pure bile salts (NaTDC or NaTC). Pancreatic lipase (20 μl) was combined with pure bile salt solutions (10 μl of either 100 mM TDC or TC in lipase buffer 2), 10 μl of substrate and 15 μl of glycerol were added to the mixture, and reactions were run for 2 hr under the same conditions described for the second system.

### Freeze fracture of lipolytic products and lipase reactions

Samples (0.5 μl) of LPs and reaction mixtures were frozen between two copper planchets (Balzers Union, Hudson, NY) either by immersion in a slush of liquid nitrogen or in a jet of liquid propane with a Balzers QFD 101 quick-freezing device. Samples were stored in polypropylene holders (31) under liquid nitrogen prior to being fractured at −120°C and $10^{-7}$ Torr in a Balzers 360 M freeze etch device. Replicas were made evaporating 2 nm of platinum (Pt) and 20 nm of carbon (C) onto the fractured surface. They were cleaned in a 40% Clorox solution for 1 hr, washed once in water, then cleaned in a solution of Chromerge (Fisher Scientific)–conc. $H_2SO_4$–$H_20$ 1:1:1 (v/v/v) for 1 hr. Five water washes preceded mounting the replica on a 200-mesh hexagonal copper grid (Ernest F. Fullam, Schenectady, NY). Replicas were viewed in a Philips 400 T electron microscope at 100 KV.

### Fish food and preparation of intestine for freeze fracture

Because luminal contents may contain vesicles from sloughed cells and fat digestion appears to involve vesiculation of lamellar lipolytic products, we designed a simple high fat food that did not contain cells or phospholipid (which would also form vesicles and further complicate the interpretation of luminal ultrastructure). The artificial food

consisted of a simple gel that contained 24.3% protein and 10.8% triglyceride (1 g of swine gelatin, 0.5 g of casamino acids, 0.670 g of olive oil, and 4.5 g of $H_2O$ sonicated at 60 W for 10–20 sec). Cubes (3 $mm^2$) were cut from the gelled mixture and five were fed to each killifish (five or six per group). Fish were killed by pithing at 30, 60, or 90 min and a sagittal incision dorsal to and intersecting the lateral midline behind the gill operculum was made. The intestine was exposed by gently pulling the head and body apart. Intestine subsamples (0.5 $mm^3$) were cut from 3-mm cross sections and immediately frozen in a jet of liquified propane.

### Freeze fracture of intestinal tissue

To process intestinal tissue, a thin layer of glycerol was applied to a rough copper planchet (Balzers planchet #BUO 12 053T) and the excised tissue was applied. A smooth dry planchet (#BUO 12 057T) was laid on top to complete the specimen sandwich. All specimens were frozen in a propane jet and processed as described above. In order to increase surface relief, samples were etched at −95°C for 3 min prior to coating with Pt/C at −140°C.

### Morphometric analysis of micrographs

Random fields were selected from at least three preparations per sample and were enlarged to a standard field size of 100 $\mu m^2$. Objects were measured with a 7X scale lupe possessing a 2-mm graticule with 0.1-mm divisions. For quantifying the number of vesicles per $\mu m^2$, at least three fields were counted and the mean of the size classes was graphed. Statistical analyses of the results were performed according to Bailey (32).

### pH of the intestine and gallbladder bile

Fish starved 24 hr, along with those fed 50 mg of the food described under fish food, were killed at 10-min intervals over a 2-hr period, and the intestine was exposed as already described. An MI 410 micro-combination pH electrode (tip diameter 1.2 mm) (Microelectrodes, Inc.) was inserted through the mouth 6–10 mm distal to the esophageal sphincter and the pH was recorded. Bile was withdrawn from excised gallbladders with a 50-$\mu l$ syringe (Supelco, Inc., Bellefonte, PA), pooled (100 $\mu l$), and the pH was measured.

### Bile salt concentration in the intestine and gallbladder

Killifish gallbladder bile contains taurocholate and cholate in a (1:1) molar ratio (26). The total concentration of bile salts in the intestinal lumen was measured indirectly after radiolabeling the endogenous bile pool with [$^3$H]taurocholate as follows. Bile was prelabeled 24 hr prior to assaying the luminal contents by feeding trace amounts ( ~ 13 ng) of [$^3$H]TC in 50 mg of food containing 20% emulsified fat (96% olive oil and 4% phosphatidylcholine) and 20% protein (10% swine gelatin and 10% casamino acids). After 24 hr, >98% of absorbed [$^3$H]TC was in the gallbladder and TLC of the bile showed that >98% of the label appeared in the TC spot suggesting that deconjugation was not occurring to any significant degree. Twenty-four hours after prelabeling the bile, fish were force-fed 50 mg of nonlabeled food and killed 15, 30, 60, and 90 min later. The gallbladder was removed, weighed, and the bile was drained onto preextracted (with $CHCl_3$–MeOH 1:1) Whatmann 3 MM filter paper (VWR Scientific, Atlanta, Ga). The paper was air-dried and extracted overnight in 5 ml of $CHCl_3$–MeOH 1:1 at 4°C. This bile salt extract was concentrated under a stream of $N_2$ and then redissolved in 2 ml of $CHCl_3$–MeOH 1:1. A 50-$\mu l$ aliquot of this extract was dried, mixed with 10 ml of Scintiverse 1 cocktail (Fisher Scientific), and counted in a Beckman LS 8100 scintillation counter (with quench correction by means of an external standard). To determine the mass of TC and cholate in the bile, 5 $\mu l$ of the bile salt extract was spotted on Chromarods and chromatographed in a chloroform–methanol–water–acetic acid 75:25:3:1 system for 20 min. Bile salts were quantified on an Iatroscan TH10 analyzer as previously described (30).

In conjuntion with these experiments, the total [$^3$H]TC activity was measured in the intestine. After gravimetrically measuring intestinal content mass, content volume was determined assuming 1 g of contents is equivalent to 1 g of water. Intestines were flushed with 5 ml of Fish Ringers buffer (33) and the flush was homogenized by freezing and thawing three times. A 0.5-ml sample was added to 10 ml of Scintiverse 1 and counted. The concentration of bile salts (BS) in the intestine could then be estimated from the equation:

mM BS intestinal contents = mM BS gallbladder bile × BS cpm/$\mu l$ intestinal contents/BS cpm/$\mu l$ gallbladder bile.

### Lipolytic products in the intestine

Luminal LPs were assayed according to the method of Honkanen, Rigler, and Patton (26). Briefly, killifish were fed 45 mg of food containing [$^{14}$C]triolein and killed at time intervals of 2, 30, 60, and 90 min post-feeding. Intestinal contents were acidified, homogenized, and extracted in $CHCl_3$–MeOH 1:1. Monoglycerides, diglycerides, and free fatty acids were quantified by TLC and flame ionization detection on an Iatroscan TH 10 analyzer as described above (26).

### CMC of cholate/taurocholate mixtures

The CMC of a 1:1 molar mixture of pure cholate and TC (i.e., simulated killifish bile) in 300 mM NaCl at pH 7.6 and 23°C was determined according to Carey and Small (34). Briefly, the shift of the maximum wavelength of absorbance for Rhodamine 6G ($2.5 \times 10^{-6}$ M) (Fisher Scientific, Norcross, GA) was monitored in a solution of

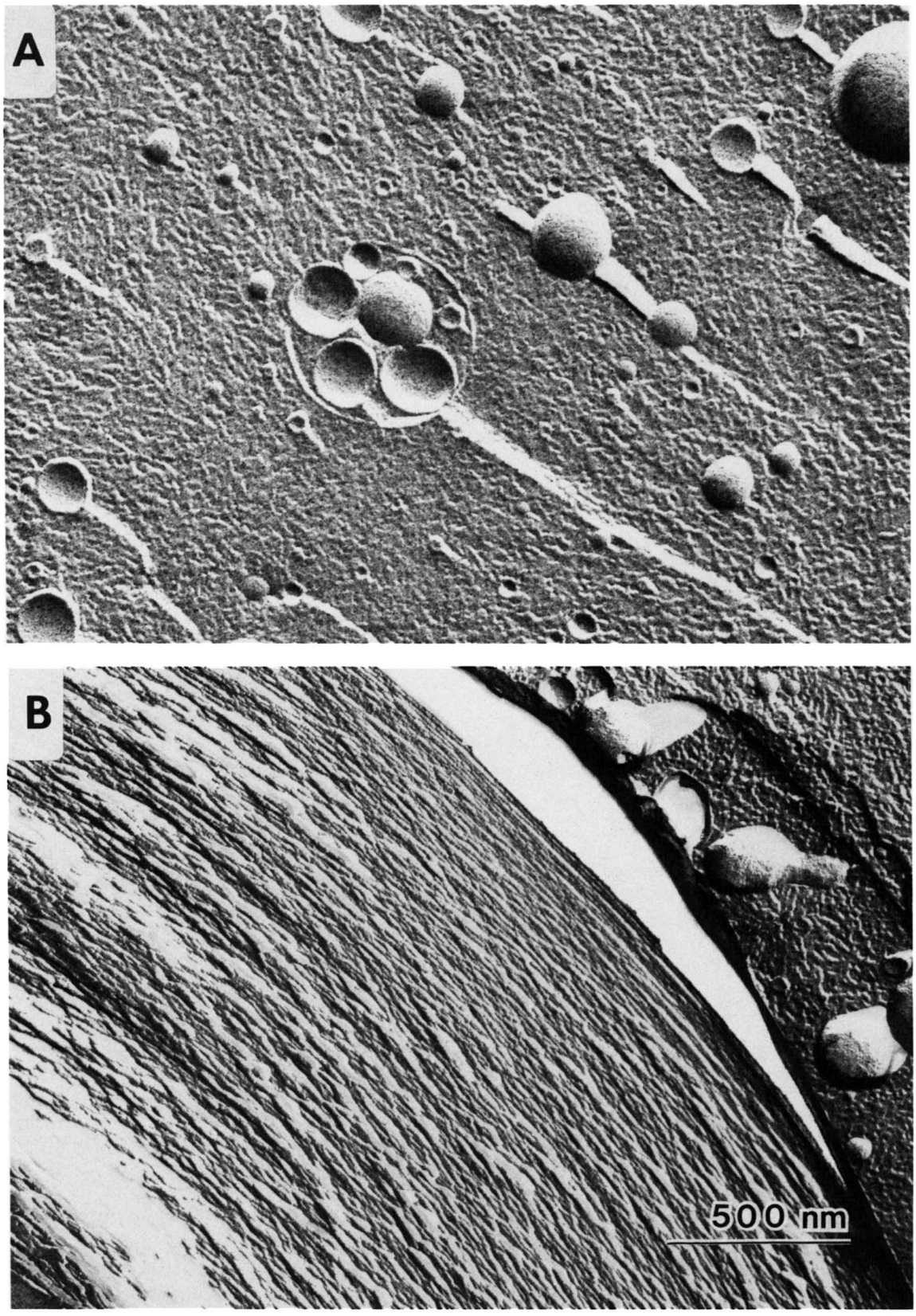


**Fig. 1.** Lamellar vesicles produced in a solution of 64 mM LPs (3:1 oleic acid:monoglyceride w/w) and 8 mM NaTDC at pH 6.9. A, A field of small dispersed vesicles; B, a large multilamellar vesicle appears in cross fracture. Both panels are the same magnification; bar = 500 nm.

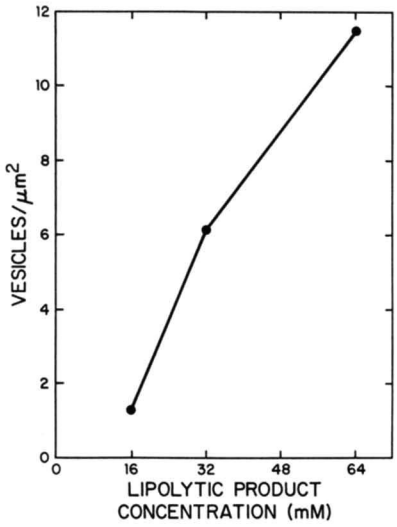


**Fig. 2.** The effect of lipolytic product concentration (oleic acid-monoglycerides 3:1, w/w) on vesicle density in the presence of 8 mM TDC by freeze fracture.

increasing total bile salt concentration (0.25, 0.5, 1, 2, 4, 5, 6, 8, 10, 15, 20, 30, 40, mM). The spectrum from 500–540 nm was manually scanned at 1-nm intervals with a model 100-40 Hitachi UV-Vis spectrophotometer. The absorbance of maximum wavelength was plotted against the log of the bile salt concentration.

## RESULTS

### Lipolytic products, model systems

Addition of pure LPs to an 8 mM TDC bile salt solution produced heterogeneous dispersions of smooth unilamellar vesicles (**Fig. 1A**). Occasionally, in solutions containing high concentrations of lipolytic products (64 mM), large multilamellar vesicles (Fig. 1B) were seen. In all preparations the number of vesicles/$\mu m^2$ was roughly proportional to the LP concentration (**Fig. 2**) and the frequency size distributions of the vesicles were similar at

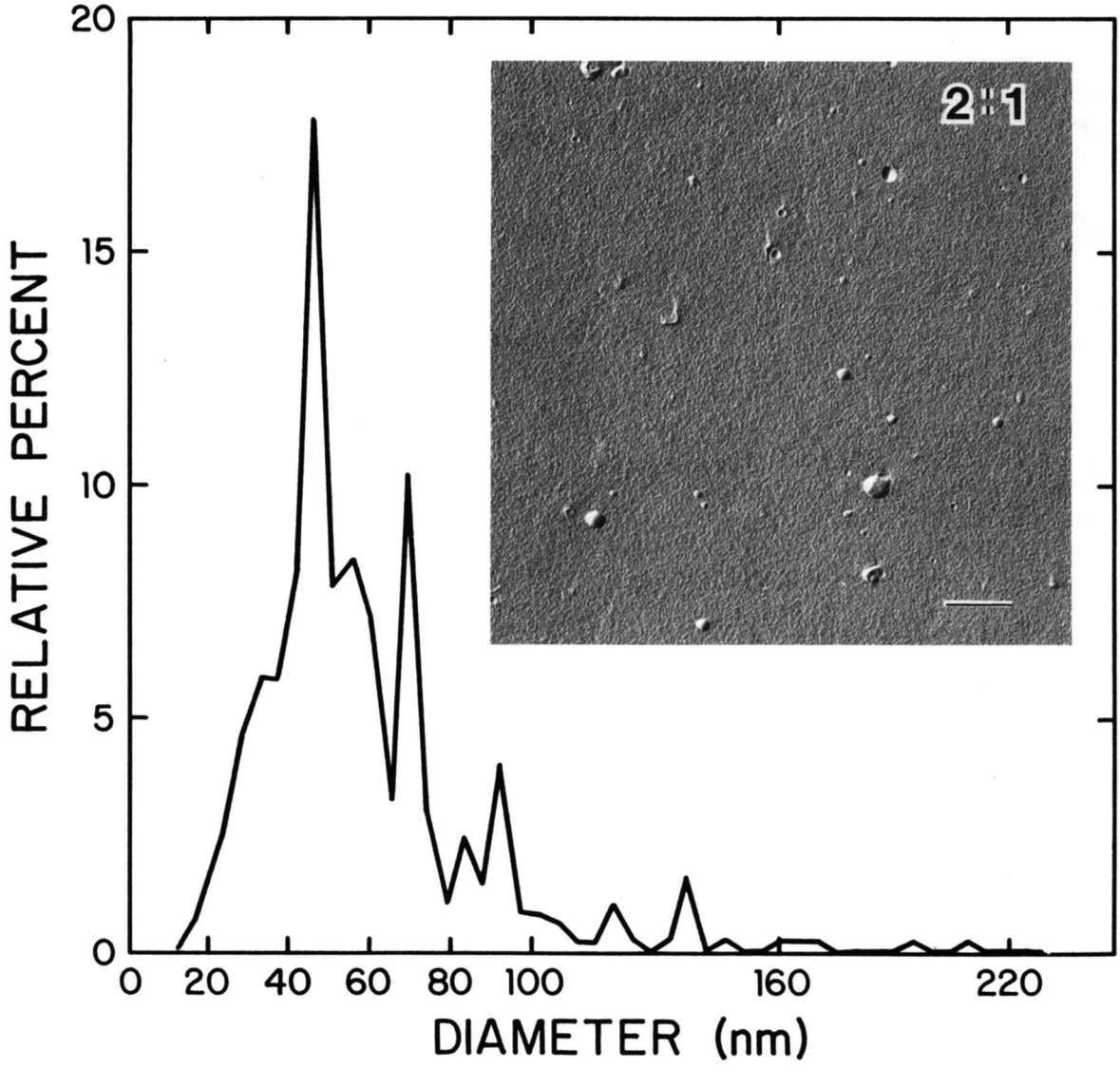


**Fig. 3.** Size distributions of product vesicles at an LP/BS molar ratio of 2 (LP = 16 mM, BS = 8 mM NaTDC) (bar = 500 nm).

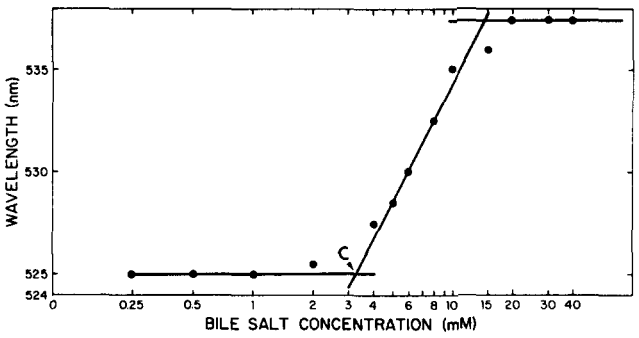


**Fig. 4.** Wavelength of the maximum absorption of Rodamine 6G versus the log of the sodium cholate-sodium taurocholate (1:1) concentration at 23°C in 300 mM NaCl. The concentration at point C is taken as the CMC of the solution.

LP/BS ratios of 2, 4, and 8. (Data shown only at LP/BS ratio of 2.) Vesicles varied in diameter (18–3000 nm) and number (up to 1200 per 100 $\mu m^2$ field at 64 mM LPs) yet none approached the resolution limit of the aqueous background (approximately 10 nm). For all preparations a large number of vesicles appeared with diameters between 23 and 60 nm (**Fig. 3**). On the average, 70% of the vesicles were in this size range (16 mM LP = 67.0%, 32 mM LP = 75.7%, 64 mM LP = 70.8%). In all preparations, major peaks of abundance occurred at 46.3, 69.5, and 92.6 nm diameters and minor peaks were seen at 11.5-nm intervals. A small percentage (<0.3%) of vesicles larger than 200 nm appeared in all preparations.

### Lipolysis in vitro

The first 30 min of lipolysis was examined chemically and ultrastructurally in a system that contained 4 mM bile salt (1:1 molar ratio of taurocholate to cholate). The critical micelle concentration of this solution was 3.25 mM using the Rhodamine technique (**Fig. 4**). **Fig. 5** shows the change in total lipolytic product during lipolysis of radiolabeled olive oil in the presence of purified lipase, colipase, and a 4 mM cholate-taurocholate 1:1 mixture. The pH decreased slightly from 7.15 to 6.94 over 30 min and nearly 5 $\mu$mol of fatty acid and 2.5 $\mu$mol of monoglyceride were produced.

By freeze fracture the first visible products of lipolysis (**Fig. 6**) appeared as spherical vesicles (arrow) at the surface of partially hydrolyzed oil droplets and in solution (arrows) after 5 min. The insert in Fig. 6 shows that the LP/BS ratio increased from ~0.7 at 2.5 min to ~ 3.6 at 30 min. In the early stages of stirred reactions (up to 5 min) at LP/BS ratios less than 1.0, few if any vesicles were seen in a field. However, after 5 min, vesicles began to appear (at least one vesicle per min/$\mu m^2$ was produced). Nearly 90% of these product vesicles were between 11 and 30 nm in diameter and only a small percentage (<1.0%) were larger than 140 nm (**Fig. 7**). Also included in Fig. 7 is a micrograph of the smallest vesicle that can be seen with this technique (arrows) along with a scale drawing of a mixed disc bile salt micelle (8) for comparison. The cutoff near 20 nm in Fig. 7 is close to the resolution limit of the technique, thus the data is artificial in the sense that smaller particles (which undoubtedly exist) are not included in the analyses.

As lipolysis proceeded beyond 10 min (**Fig. 8A**), lamellar product (arrows) accumulated at the surface of oil droplets. This was indicated by the appearance of droplets possessing convex or concave fracture faces and the disappearance of cross-fractured droplets. Some of the partially digested droplets possessed a granular matrix which covered the undigested oil of the core (Fig. 8B). In the final stages of lipolysis (Fig. 8C), some product appeared as multilamellar vesicles (arrows) possessing aqueous layers as shown by prolonged etching (1.5 min) to remove water.

Similar lipolytic products were seen in other systems containing different bile salts. When lipolysis in the presence of 17 mM TDC or 17 mM TC was allowed to proceed for 2 hr at pH 6.8 (**Fig. 9A**), multilamellar product phases (LA) accumulated and lamellar product vesicles (VE) (50–250 nm) could be seen originating from the lamellae. When fresh pig pancreatic juice was incubated with an olive oil emulsion in the presence of 42 mM pig gallbladder bile for 2 hr, similar results were seen (Fig. 9B). In contrast to the model LP system where smooth spherical vesicles were observed, the vesicles seen during lipolysis were often irregular in shape.

### Lipolysis of the fat meal in vivo

**Table 1** shows the concentration of luminal bile salts, lipolytic products, and the LP/BS molar ratio in killifish intestinal contents. Within the first 30 min, 50% of the TG was converted to products (monoglycerides, diglycerides, and free fatty acids). The between-meals bile salt concentration of 1.07 mM increased 9 times over a period of 30 min and reached nearly 30 mM after 90 min. The LP/BS ratio dropped from 8.5 immediately after feeding

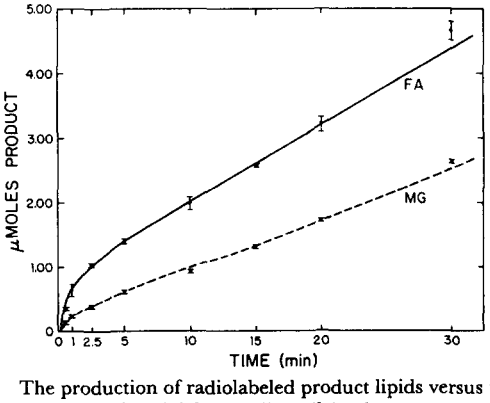


**Fig. 5.** The production of radiolabeled product lipids versus time during the hydrolysis of radiolabeled olive oil in the presence of purified pancreatic lipase, colipase, and a 4-mM bile salt mixture of cholate and taurocholate (1:1). FA, free fatty acid; MG, monoglyceride.

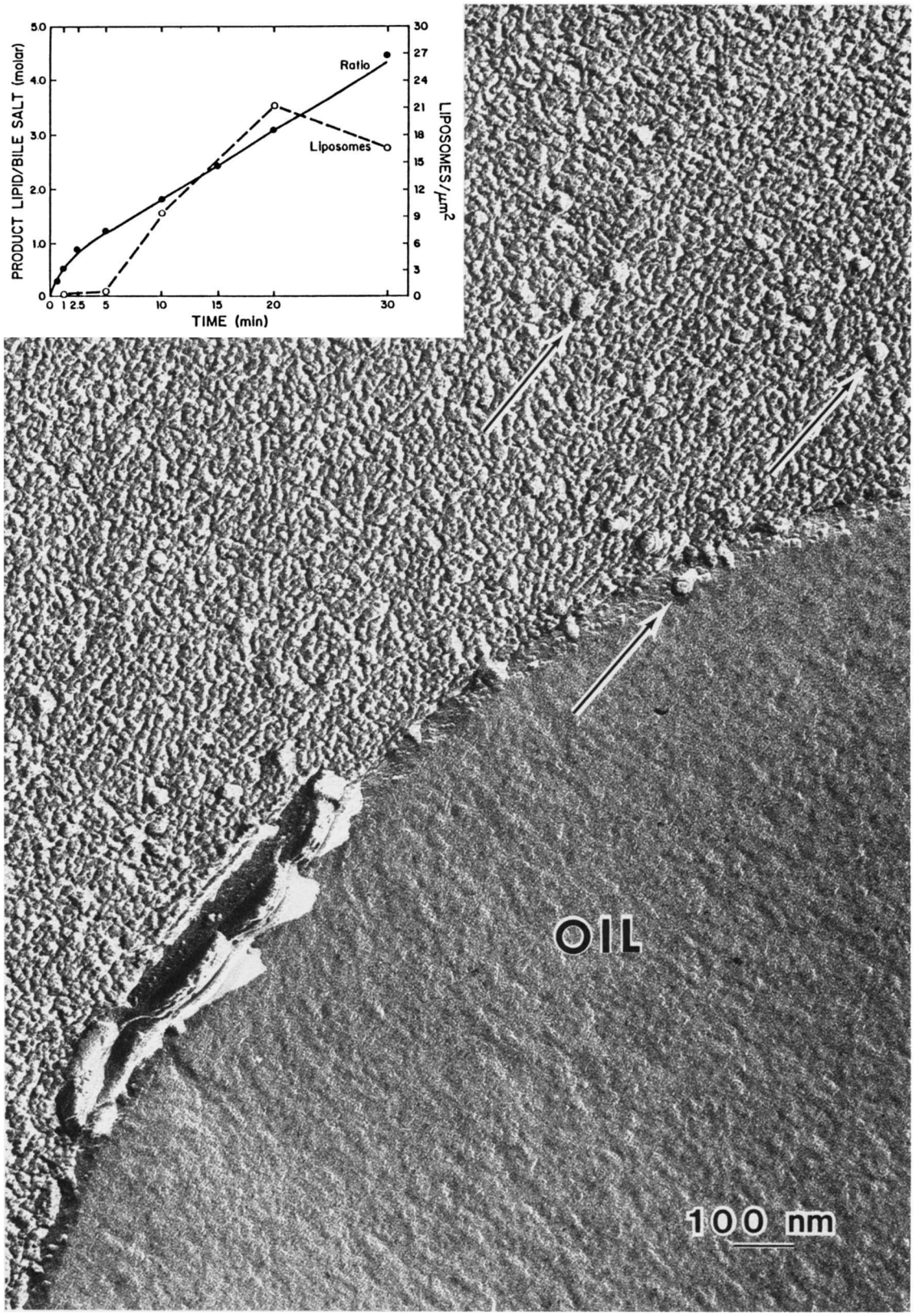


**Fig. 6.** Morphology of the LPs generated in Fig. 5. Production of product lamellae and vesicles at the surface of a large oil droplet (arrows) 10 min after the addition of enzyme. The LP/BS ratio and vesicle (liposomes) production over a period of 30 min are shown by the insert.

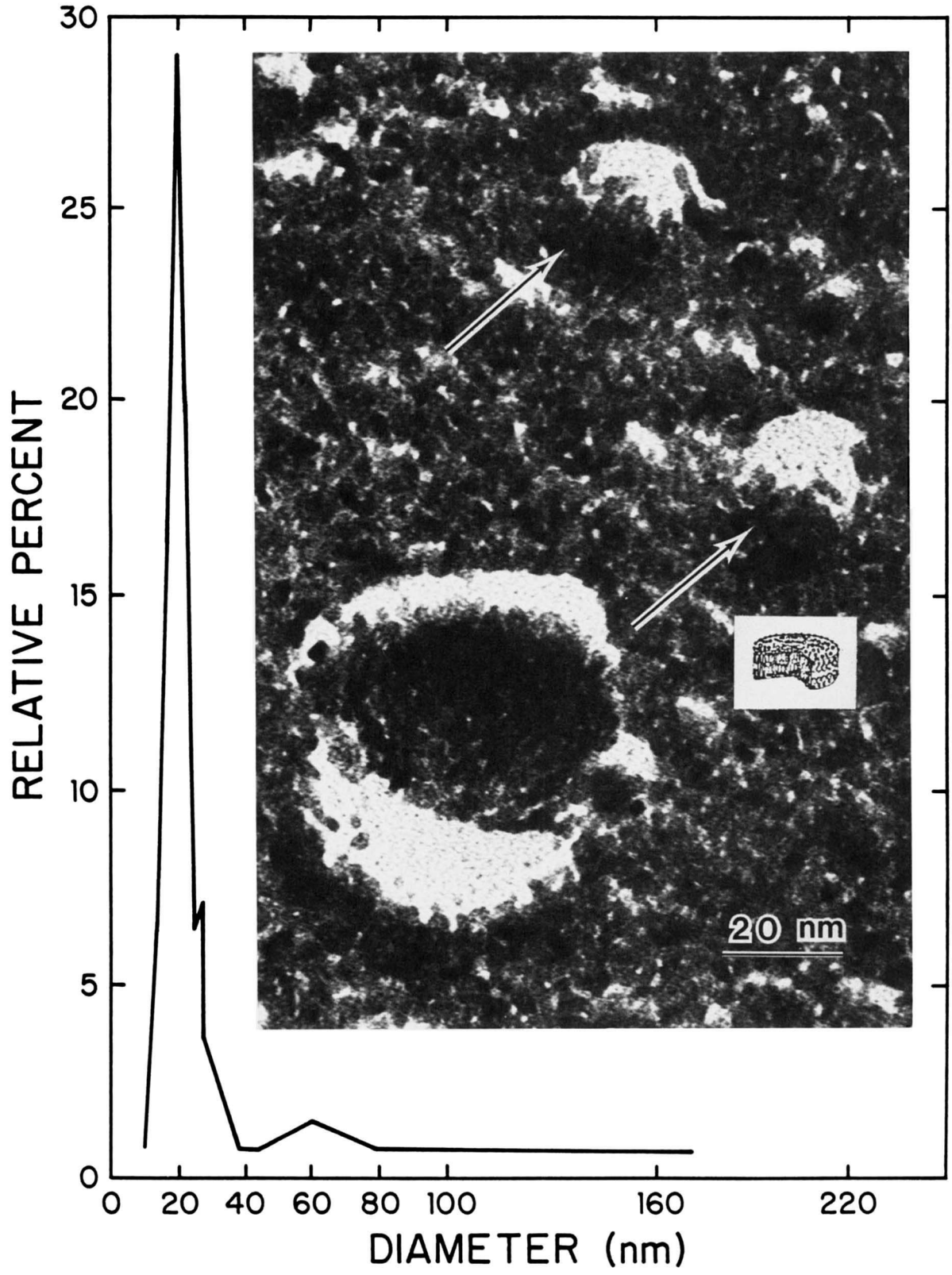


**Fig. 7.** Size distributions of vesicles seen in Fig. 6 and extreme magnification of the smallest visible vesicle with a scale drawing of a mixed lipid micelle (8) 15 nm in diameter. Arrows indicate spherical vesicles which project out of the plane of the page. The granular background is made up of platinum grains 2–4 nm in size.

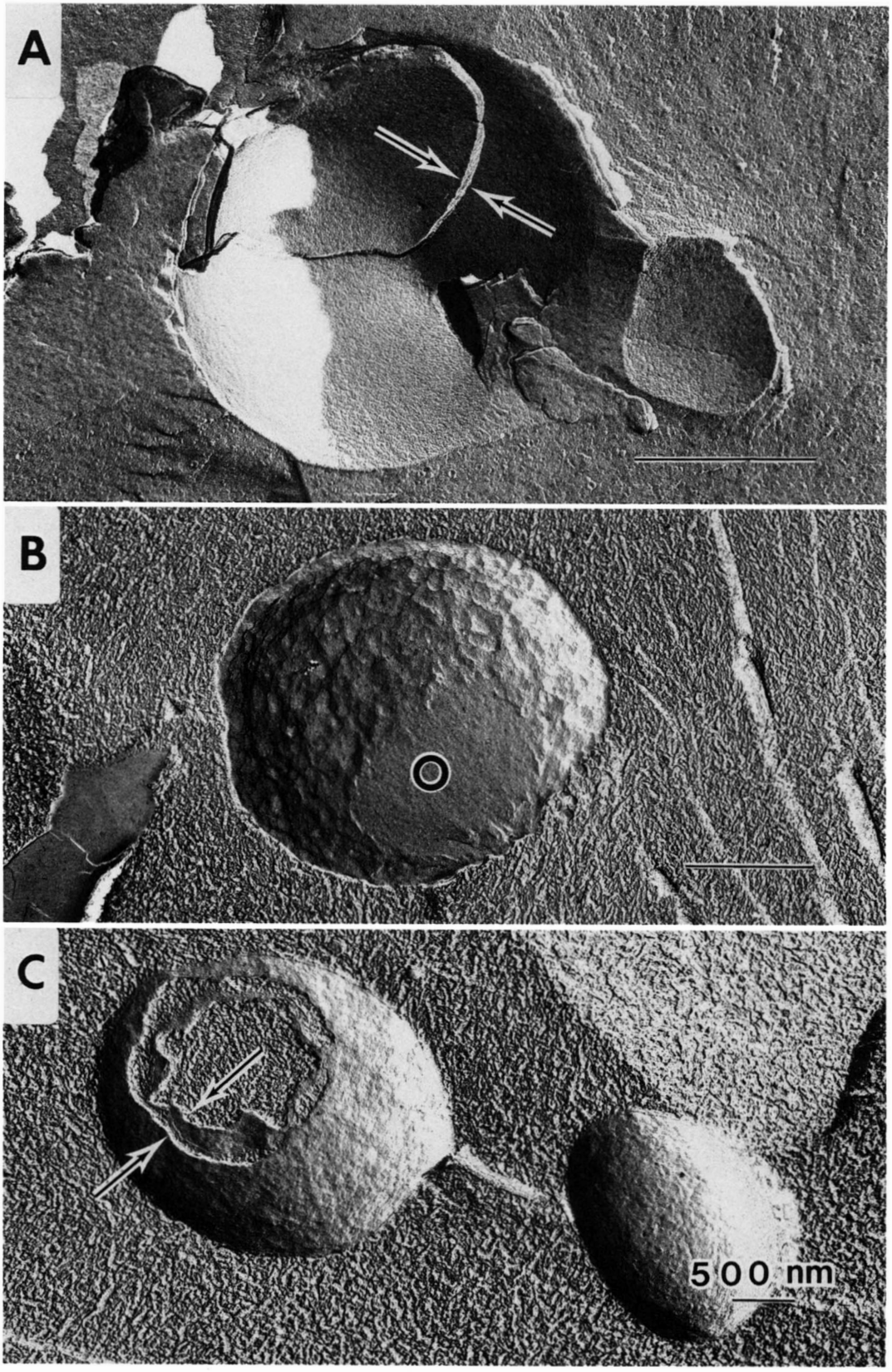


**Fig. 8.** Product lipid as in Figs. 6 and 7. A, Multilamellar product vesicle 10 min after the addition of lipase; B, partially digested triglyceride droplet (at 10 min) showing an oil core (O) and rough textured surface; C, etched (3 min) product vesicles as in A, showing an aqueous core and lamellae (bars = 500 nm).


**Fig. 9.** LP morphology of two systems containing lipase, bile salts, and triglyceride in which lipolysis was allowed to go to near completion (2 hr). A, Product lamellae (LA) and vesicles (VE) produced by action of pancreatic lipase on triolein in the presence of 17 mM taurodeoxycholate. B, In the presence of 42 mM pig gallbladder bile and pig pancreatic juice, vesicles and lamellae also appear (see Methods for details).

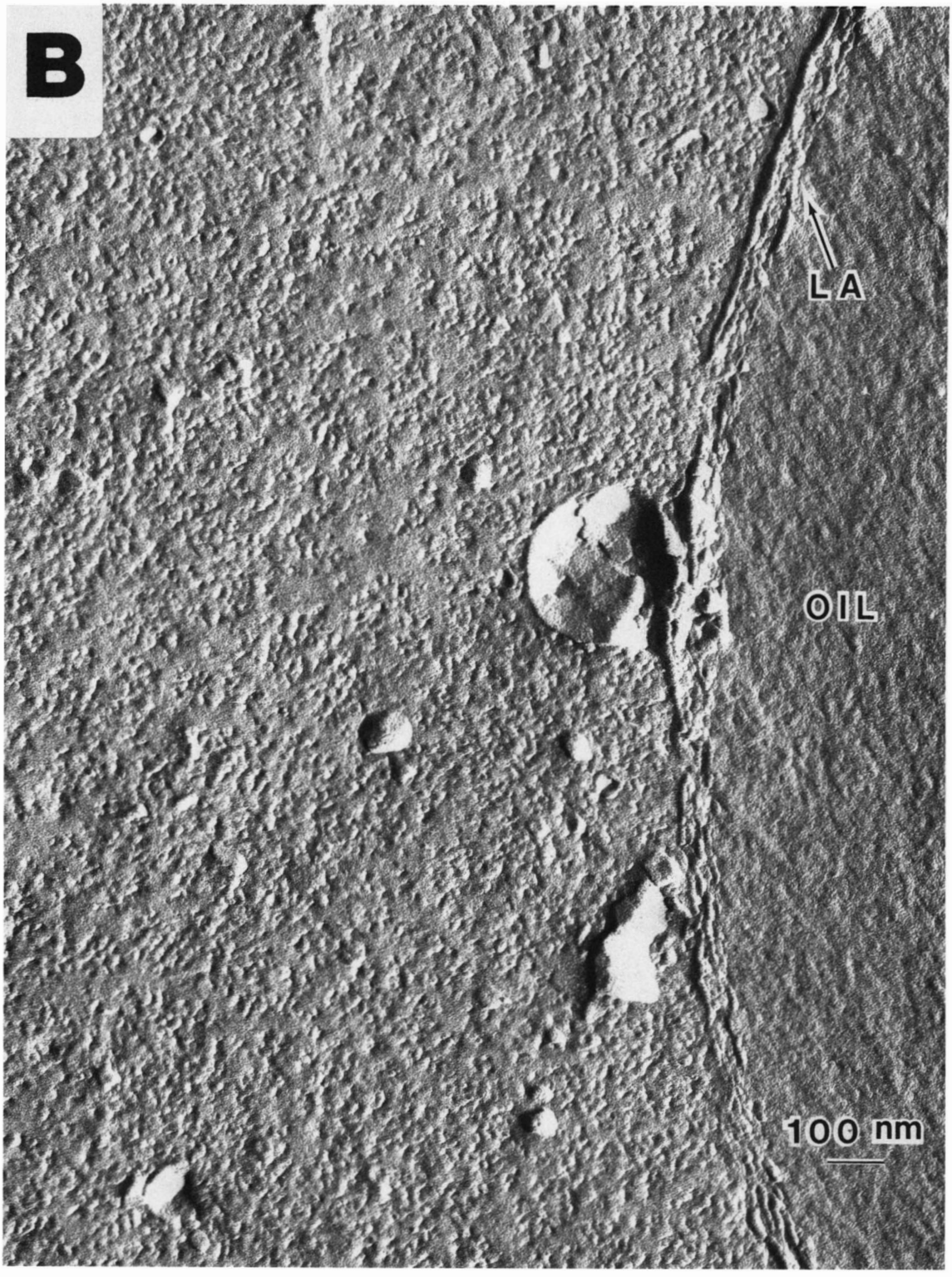


to 1.00 after 90 min. The pH of the intestinal fluid in unfed fish was 8.58 ± 0.16 (n = 10) and that of the bile was 7.50 ± 0.09. After a 10% fat meal, the average pH of the gut contents dropped to 7.58 ± 0.19 after 1 hr.

The morphology of the lipid product phases in the killifish intestine after a 10% fat meal is shown in **Fig. 10** and **Fig. 11.** After 30 min, masses of rough multilamellar product phases were found in intestinal contents (Fig. 10A

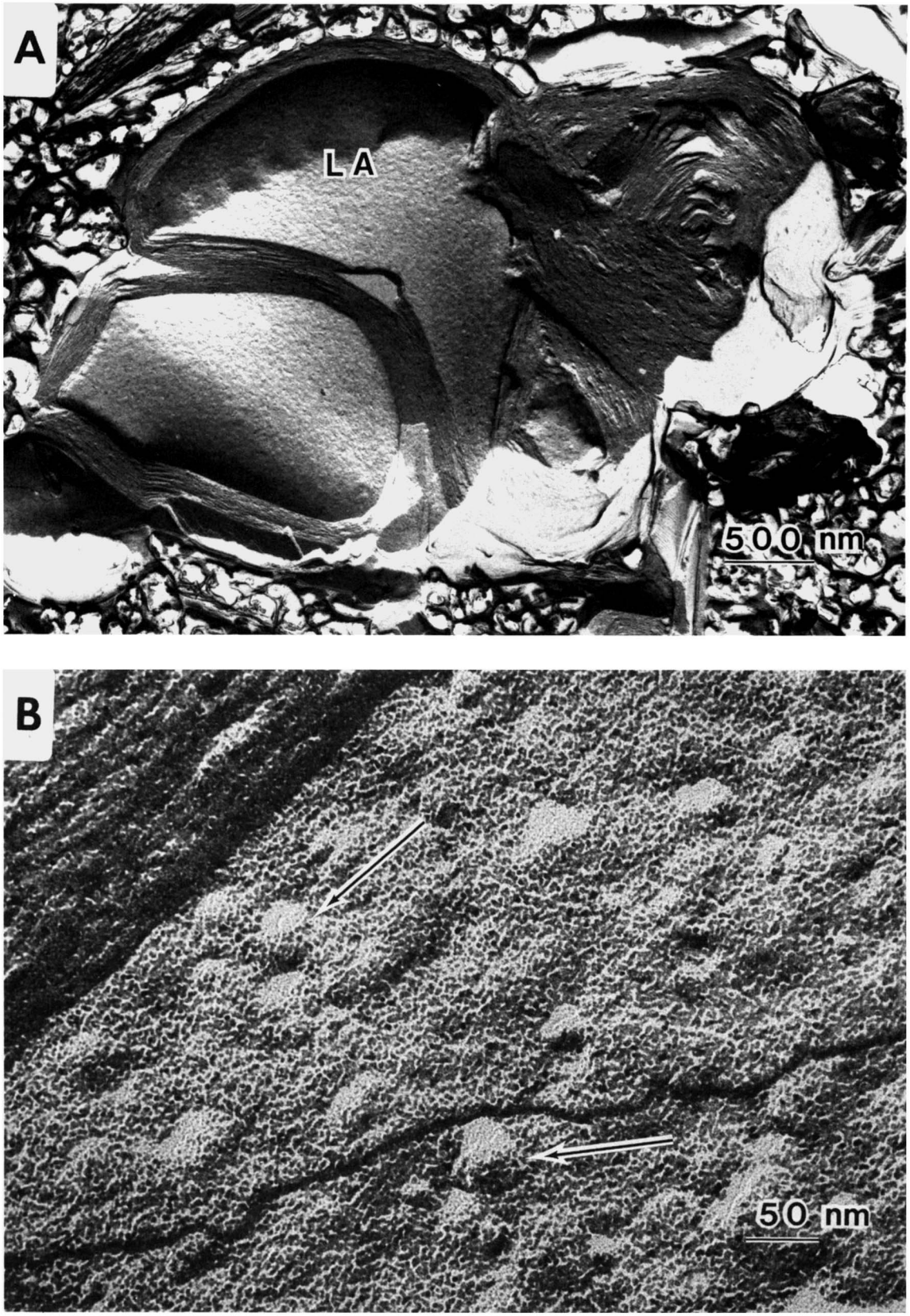


**Fig. 10.** The morphology of the product lipids in the killifish gut contents over 90 min. A, At 30 min, masses of rough lamellar product lipid (LA) fill the lumen; B, high magnification of rough lamellae as in A. C, Product lamellae do not accumulate on partially digested oil droplets after 60 min, indicating that the bile salts released from the gallbladder are solubilizing the excess lipid. Lipolytic product at the oil-water interface is shown by arrows. D, An oil droplet after 90 min with lamellar and vesicular products (bars = 500 nm).

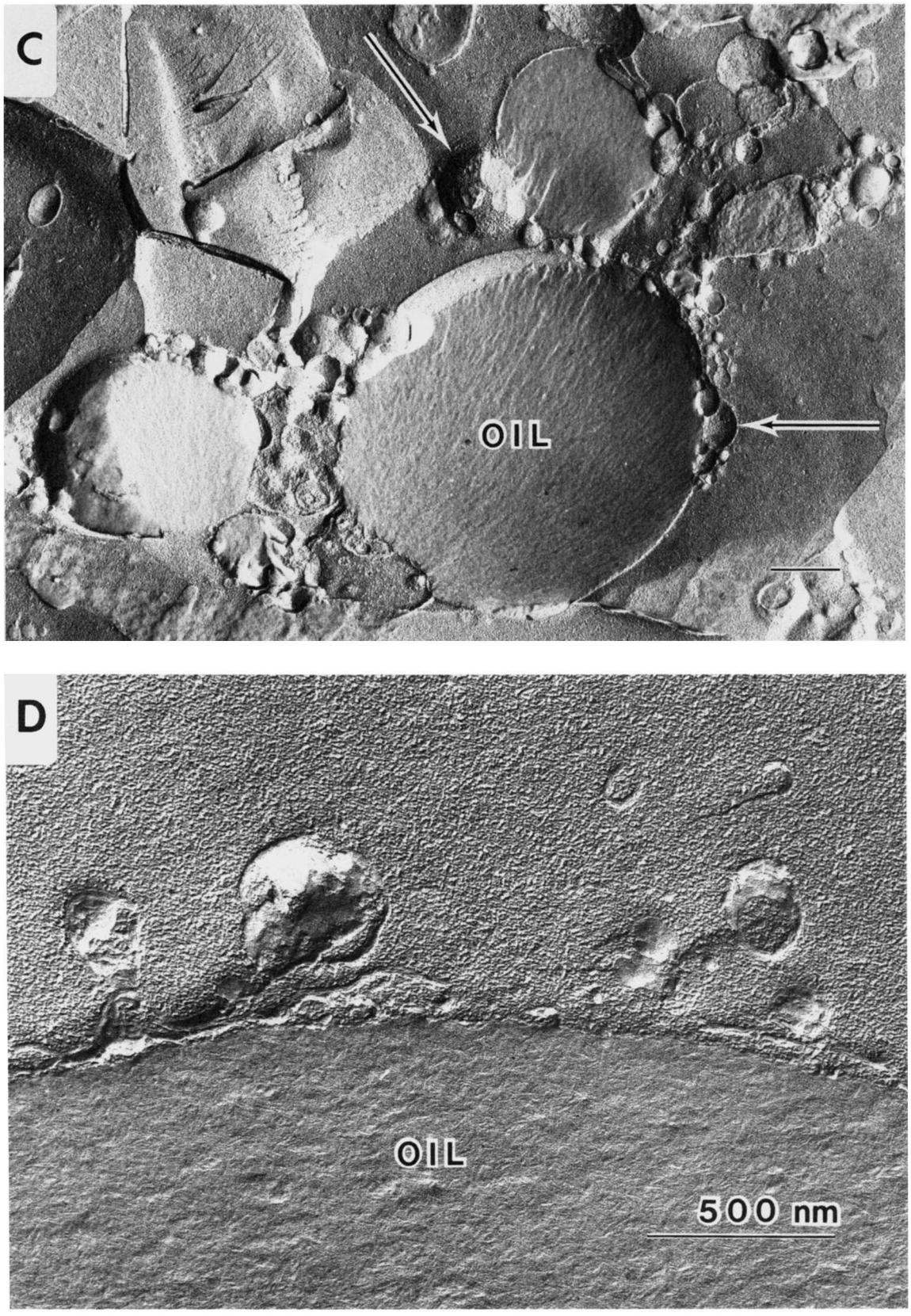

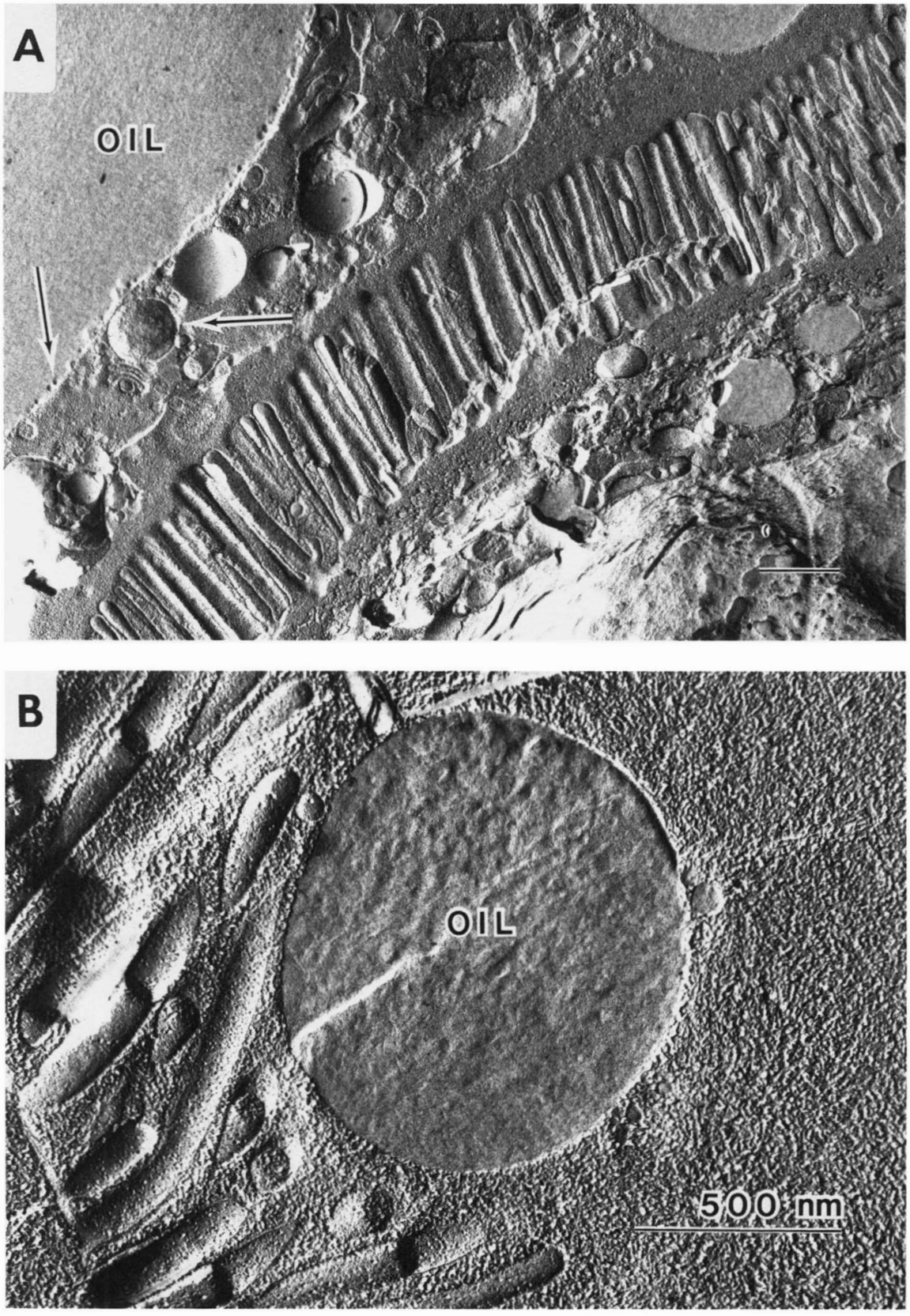


**Fig. 11.** The morphology of fat digestion in the lumen of the killifish gut after a fat meal. A, Lamellar product vesicles (arrows) are dispersed from the perimeter of a large oil droplet (upper left) near an enterocyte (lower right); B, a vesicle and unhydrolyzed oil droplet nearly touch the brush border during lipolysis (bars = 500 nm).

TABLE 1. Concentrations of bile salts and lipolytic products[a] in the gut of the killifish following fat feeding

| Time | Bile Salt | Lipolytic Products | Lipolytic Product/Bile Salt |
|---|---|---|---|
| *min* | *mM* | *mM* | *molar ratio* |
| 2 | 1.07 | 9.10 | 8.50 |
| 30 | 9.27 | 34.50 | 3.72 |
| 60 | 18.04 | 66.00 | 3.66 |
| 90 | 29.99 | 30.00 | 1.00 |

[a]Free fatty acids, monoglycerides, and diglycerides.

and B). Fig. 10B shows a high magnification of the multilamellar product phases seen in the intestine. Numerous bumps (arrows) appear to give the lamellae a rough irregular texture. After 60 min, product appeared as lamellar vesicles (arrows) arising from the surface of partially hydrolyzed TG droplets (Fig. 10C and D). Large numbers of product vesicles and TG droplets were observed in the intestine. Product lipid was seen radiating from the perimeter of large TG droplets (Fig. 11A) in close proximity to enterocytes. In Fig. 11B an unhydrolyzed oil droplet appears within 100 nm (0.1 $\mu$m) of the brush border. During digestion and absorption of a fat meal in vivo, no fusion of product vesicles to microvilli was ever observed.

### Lipolysis between meals in vivo

Killifish intestine absorbs dietary fat rapidly but may take several days to secrete a large dose of absorbed fat into the circulation (26). Normal sloughing of cells laden with fat and lipoproteins occurs at all times including between meals when submicellar bile salt concentrations are present in the intestinal lumen (see, Table 1 at 2 min). **Fig. 12A** shows multilamellar lipid associated with microvilli (arrows) 24 hr after a fat meal when luminal BS concentrations are submicellar but sloughed cells still contain large fat vacuoles. In addition, fish intestinal very low density lipoproteins (25) from sloughed cells also appear in the lumen. Figs. 12B and C show "packets" of small homogeneous VLDL (41 ± 0.97 nm) between (arrow) and within (not shown) the cytoplasm of enterocytes. In Fig. 12D, VLDL are seen (arrows) in the lumen after being released from a sloughed enterocyte.

### Particle sizes in luminal contents

A size distribution of all types of vesicles from the intestinal lumen of a fat-fed killifish is shown in **Fig. 13**. Nearly 90% of the particles possesses a diameter between 20 and 100 nm and only a small amount (4%) was larger than 150 nm. For comparison, the average diameter of blebbing killifish microvillus membrane vesicles and trout VLDL (25) is shown.

## DISCUSSION

From model in vitro systems to systems in vivo this study shows that, in the presence of micellar bile salts, lipolytic products (LPs) appear in the form of vesicles as the LP/bile salt molar ratio increases beyond 1.0. At higher LP/bile salt ratios, LPs form multilamellar phases. **Fig. 14** schematically depicts the accumulation of product lamellae and their dispersion into vesicles. Micellar structures were not visible by the techniques used in this study (see below). The density of the lamellar lipolytic product phases appears to vary depending on the LP/BS ratio and the presence or absence of divalent salts (3). At high LP/BS ratios, LPs appear to float with triglyceride following centrifugation, while at low LP/BS ratios the density of LP structures increases and they may remain in the supernatant (3). Thus, a real separation of the varied phases of fat digestion in intestinal content by centrifugation or ultrafiltration will be impossible. The results of this study suggest that measurement of the concentrations of lipids and bile salts in intestinal content alone, coupled with the knowledge of the phases formed at different ratios (and at different unbound divalent salt concentrations), will evenually enable one to accurately predict the state of lipids in intestinal content.

A summary of the characteristics of the multilamellar phases that were observed in this study under a variety of conditions is shown in **Table 2**. Lamellae that accumulated on partially hydrolyzed TG droplets varied from 4 to 16 nm in thickness and were separated by a water layer in some cases (Fig. 8C). Lipid layers produced in the presence of pure bile salts were twice as wide as those produced in the presence of mixed bile salt solutions (Table 2). Although with longer incubations times the distance between individual lamellae increased, all lamellae appeared to have rough irregular surfaces. Recently, Müller (8) determined that the thickness of bilayers produced on particles composed of lecithin–bile salts 3:1 was 5.1 nm and, in an earlier model, Small (35) estimated that micelle discs were 5 nm in cross section. In general, the molecular architecture of lamellar phases varies depending upon the total water content and lipid species present.

In systems containing monoglycerides and water, NMR and X-ray diffraction data show that lamellae are produced which possess a dynamic cubic structure depending on the lipid/water ratio (36–38); however, the freeze fracture morphology of the cubic phase has been disputed (39). Whether or not the rough multilamellar structures seen by freeze fracture in this study actually possess a cubic configuration is uncertain. Clearly, the layered phase is an intermediate in fat digestion in vivo and undoubtedly corresponds to the "viscous isotropic phase" seen by light microscopy (3). Layered phases are also seen when oleic acid is freeze fractured (40), and Eins (41) has shown that lamellae with repeat distances of 3.69

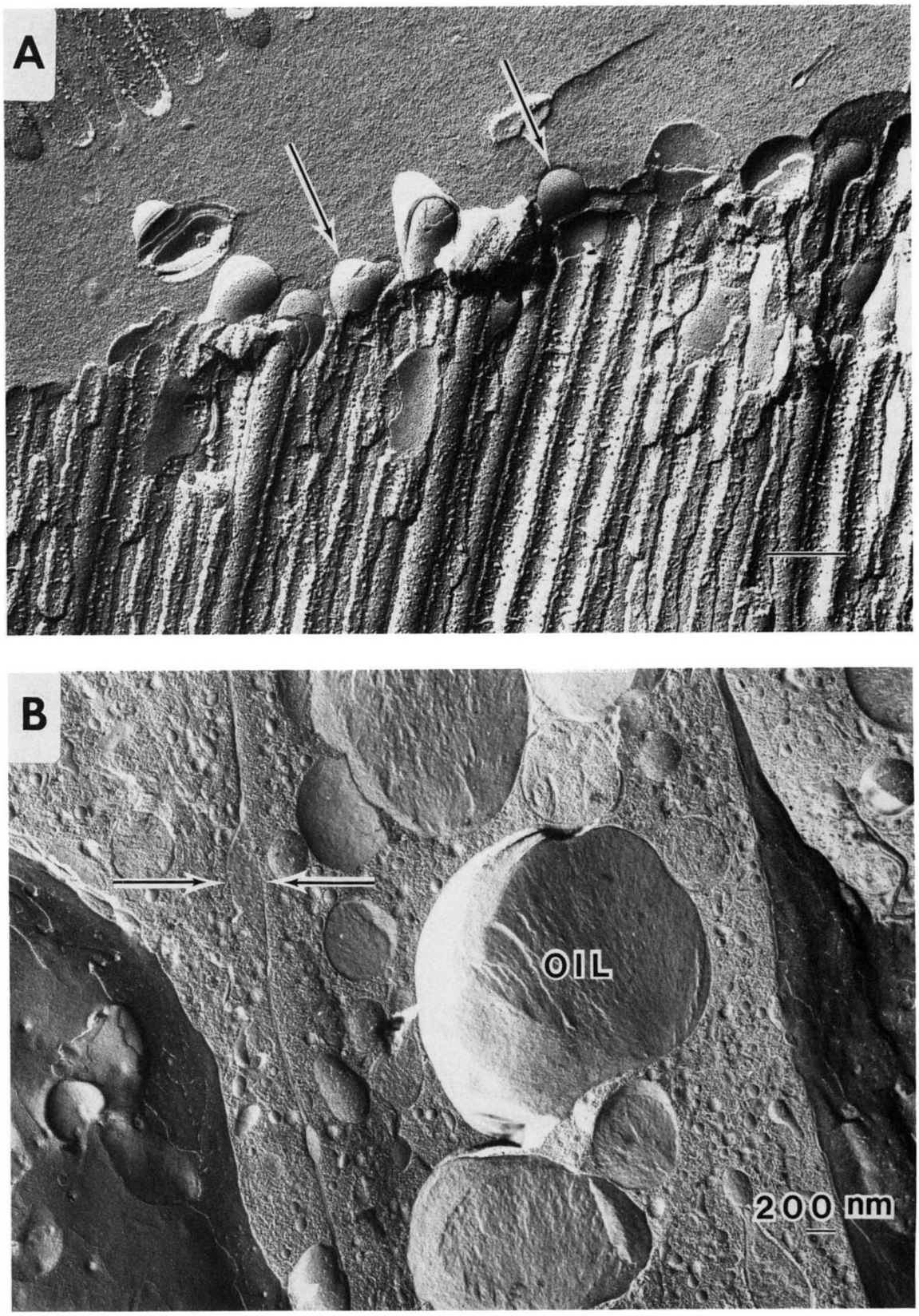


**Fig. 12.** Endogenous lipid in the intestine of the killifish. A, Lamellar endogenous lipid at the brush border (arrows). B, "Packets" of lipoprotein particles are seen between enterocytes (arrows in B) and at high magnification in C. In D, a vesicle dispersion (probably from a lysing cell) is shown in the intestinal lumen. Arrows indicate lipoprotein particles (bar = 200 nm).

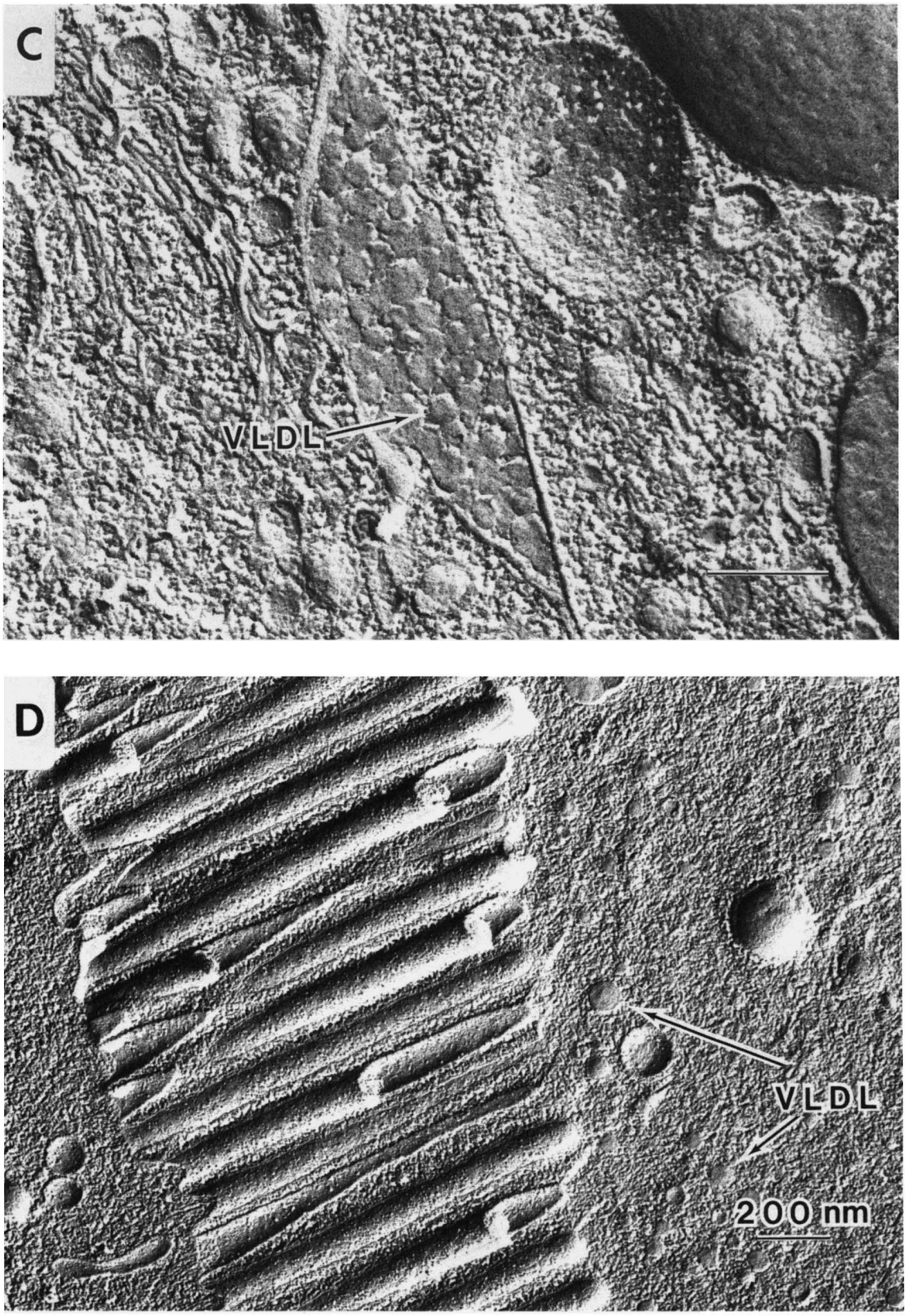

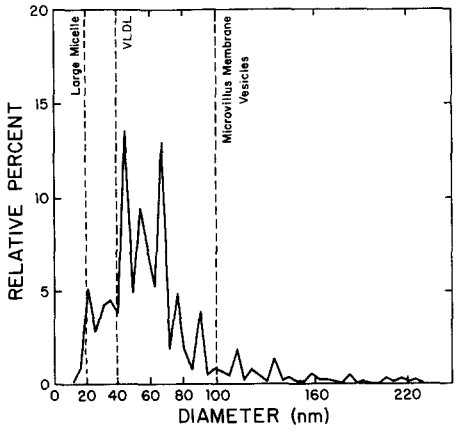


**Fig. 13.** Size distribution of luminal vesicles from the intestine of the killifish 60 min after a fat meal. The size of large mixed lipid micelles along with the size of microvillus membrane vesicles and killifish VLDLs are shown.

nm are produced from the potassium salts of oleic acid in water. Also, water can penetrate and separate multiple lipid layers. It has been shown that water penetrates aracidonic acid layers and produces a concentration gradient which is high at the surface but rapidly diminishes within the first 10 layers (42). This phenomenon, along with continuous vesiculation and micellarization of product lamellae by bile salts, may help explain the lamellar thickness variations seen in our systems.

At high LP/BS molar ratios (>5:1), a reversed micellar L2 phase consisting of water layers interspersed between non-lamellar lipid layers may occur. This non-lamellar phase has been visualized by freeze fracture, but only in equilibrated monoglyceride-water systems (43). Lindström et al. (44) have also tentatively identified the L2 phase by X-ray diffraction in a physiologically relevant system containing oleic acid and monoolein (2.5% w/w,

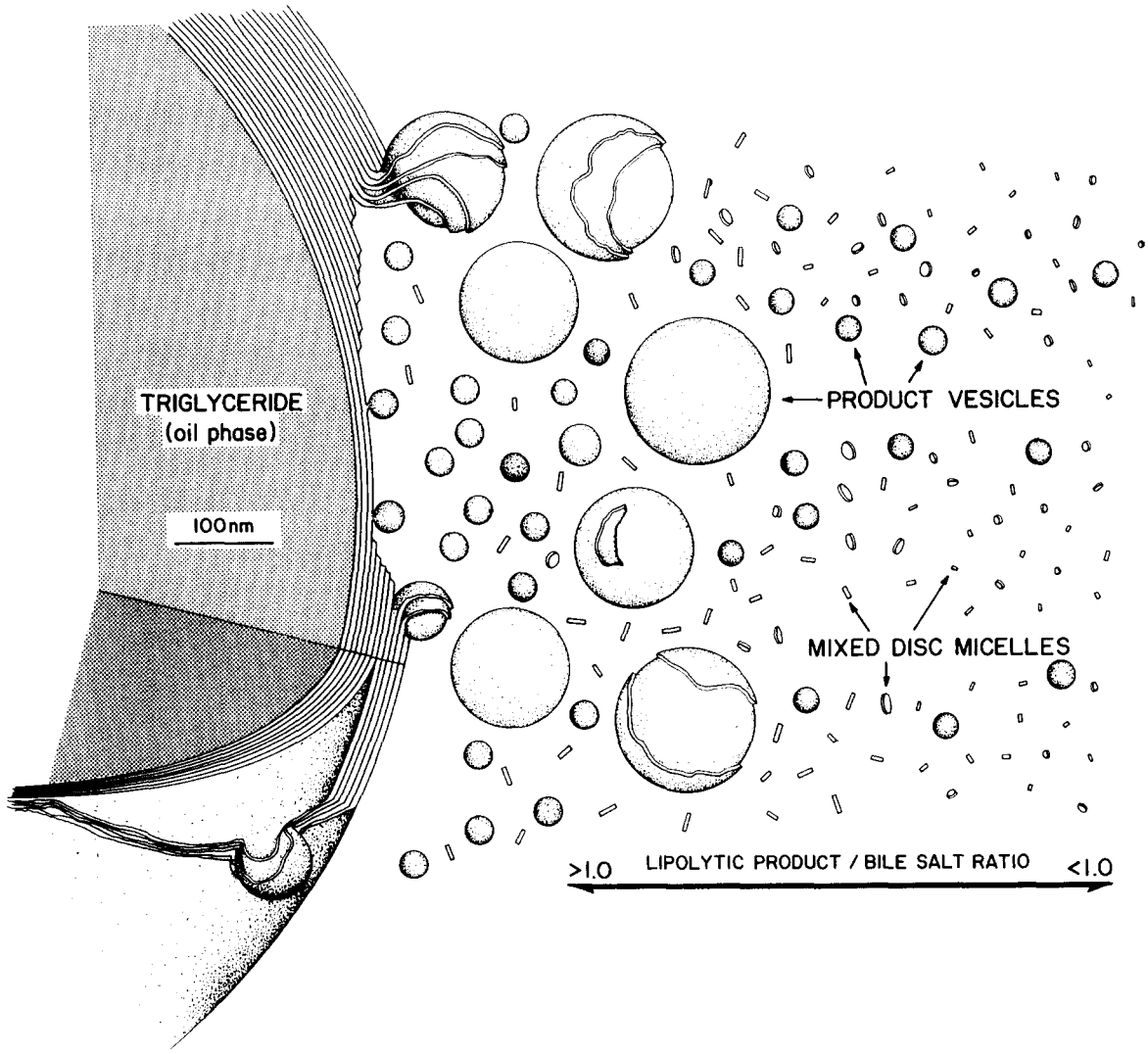


**Fig. 14.** Accumulation of product lamellae and their dispersion into vesicles.

2:1 molar ratio), 150 mM NaCl, and 10 mM TDC at pH 6.5. The LP/BS ratio of Lindström's system was aproximately 10:1 and the lipid phases were concluded to be non-lamellar. Our model system containing 64 mM LPs possessed an LP/BS ratio of 8:1 and was nearly identical in composition to that of Lindström et al. (44), yet only lamellar lipid phases were seen. High LP/BS ratios were produced during lipolysis in vitro and in the gut of the killifish after a fat meal and, again, only lamellar phases were seen. From these results we conclude that the L2 phase may not occur or is transitory during the dynamic process of lipolysis.

The bile salt micelle is essential for the solubilization and dispersion of lipolytic products in the intestine. Although the shape of simple bile salt micelles is thought to be spherical (45), the addition of LPs or phospholipids causes them to grow in diameter and become disc-like until the micellar phase boundary is reached. When the boundary is reached, spherical vesicles appear and coexist with the disc shaped micelles (46). In lecithin/bile salt systems, the boundary can occur at LP/BS ratios of 0.4 or greater (9). Below the mixed lipid/bile salt phase boundary, model systems containing phospholipids, cholesterol, triglyceride hydrolyzates, and bile salts produce disc-like micelles with a mean diameter of 40 nm (46). Above this phase boundary, spherical lamellar vesicles are also produced. Mazur et al. (9) have shown by laser light scattering and negative staining TEM that the diameter of disc-shaped lecithin/taurocholate micelles increases rapidly (from 3.5 to 20 nm) as the lecithin/TC ratio is increased from 0.42 to 0.85. In the present study, when LP/BS molar ratios exceeded 1.0, lamellar vesicles were produced, which agrees with NMR (8) and laser light scattering data (9). However, disc-shaped micelles could not be discerned. When disc-shaped bilayer micelles (35) split in the middle of the bilayer during freeze fracture, then a disc micelle 40 nm in diameter might be seen by freeze fracture if the plane of the disc lay parallel to the plane of fracture. If the disc were oriented perpendicular to the plane of fracture, a thin line (up to 40 nm long) the thickness of a typical bilayer ($\sim$5 nm) might be seen. The inset in Fig. 7 shows a scale model of a 15-nm disc micelle. Note also the size ($\sim$ 2-4 nm) of the black platinum grains that make up the bulk of the replica. These grains can be seen individually around the large vesicle in the lower left corner of Fig. 7. Either mixed disc micelles do not provide sufficient relief to perturb the blanket of platinum grains, or their size is smaller than has been predicted by light scattering studies (9, 46). With better resolution, they would probably be seen.

The smallest visible LP/BS structures seen in this study are shown in Figs. 6 and 7 (arrows). These apparently globular structures lie at the resolution limits of the replicas' aqueous regions ($\sim$ 10 nm) and their average diameter (23.8 nm) is nearly half the size of the putative large mixed disc micelle (46). These results suggest that either the lower size limit for LP/BS bilayer vesicles is approximately 20 nm or else there is some other structure to this particle that is neither disc-like nor bilayer-like. Possibly, this particle may be similar in structure to the spherical particle composed of bile salt and lecithin proposed by Müller (8).

The killifish were fed a simple high fat food in order to simplify interpretation of luminal ultrastructure. In the environment, killifish are aggressive opportunistic carnivores whose diet is varied and complex (47, 48). High fat food items in their diet include certain larvae, gonads of their prey, and the planktonic oil-filled eggs of many spe-

TABLE 2. The thickness of lipolytic product lamellae from four different preparations in the presence of bile salts

| Preparation | Lipid/Bile Salt | Lamellae Thickness and Range |
|---|---|---|
| | *molar ratio* | *nm* |
| Oleic acid monoglyceride (3:1) + 8 mM taurodeoxycholate, 2 hr after mixing | 8.0 | 11.1 ± 4.64 (n = 52) 3.3-13.9 |
| Olive oil emulsion + lipase extract + 17 mM taurodeoxycholate, 2 hr incubation | 53.0[a] | 10.0 ± 1.50 (n = 54) 7.6-11.9 |
| Olive oil emulsion + pure lipase/colipase + 4 mM cholate/taurocholate, 30 min incubation | 6.0 | 5.7 ± 0.82 (n = 12) 5.0-6.6 |
| Killifish intestine contents + olive oil emulsion + native bile salts, 30 min incubation | 9.0 | 4.3 ± 0.26 (n = 47) 4.0-4.6 |

[a]Assuming 90% hydrolysis.

cies. Thus, although our artificial food was unrealistic in some ways, it was avidly consumed and absorbed by the fish and did not necessarily contain more fat than a meal of oil-rich fish eggs. After 90 min, 70–80% of the fat in the meal was absorbed, the gallbladder emptied causing a rise in the bile salt concentration from 1.0 to 30 mM, and lamellar lipolytic products were observed. With a low fat meal, lipolytic products might not have been seen. Unfortunately, the presence of sloughed cells in the lumen, which vesiculate as they are digested, can make identification of small lipolytic product vesicles by electron microscopy extremely difficult.

In conclusion, this study indicates that lamellar lipolytic products are intermediate phases during fat digestion (49) only when the lipolytic product/bile salt molar ratio exceeds 1.0. Clearly, whether or not this ratio is exceeded in vivo depends on numerous factors including the level of fat in the diet, the way it is dispersed in the food, and the health of the organism. Following a fatty meal in humans, the LP/bile salt ratio exceeds 1 (6, 7). Thus, lipolytic product lamellae and vesicles would be expected to occur as intermediates in fat digestion in humans.

This work was supported by grants from the National Institutes of Health, 5-R01-AM27304-05 and RCDA AM01076-03 to JSP, along with a small grant from the Georgia Research Foundation. Special thanks go to Drs. H. A. Dailey, I. L. Roth, and J. Paulin for review of the manuscript, Pat Bates for excellent word processing, and to all the helpful individuals at the University of Georgia Center for Ultrastructural Research.

*Manuscript received 17 June 1985.*

## REFERENCES

1. Hofmann, A. F., and B. Börgstrom. 1962. The intraluminal phase of fat digestion in man: the lipid content of the micellar and oil phases of intestinal content obtained during fat digestion and absorption. *J. Clin. Invest.* **43:** 247–257.
2. Hofmann, A. F., and B. Börgstrom. 1962. Physical-chemical state of lipids in intestinal content during their digestion and absorption. *Federation Proc.* **21:** 43–52.
3. Patton, J. S., and M. C. Carey. 1979. Watching fat digestion. *Science.* **204:** 145–148.
4. Rigler, M. W., and J. S. Patton. 1983. The production of liquid crystalline product phases by pancreatic lipase in the absence of bile salts. A freeze fracture study. *Biochim. Biophys. Acta.* **751:** 444–454.
5. Mazur, N. A., and M. C. Carey. 1983. Quasielastic light scattering studies of aqueous biliary lipid systems. Cholesterol solubilization and precipitation in model bile solutions. *Biochemistry.* **22:** 426–442.
6. Stafford, R. J., and M. C. Carey. 1981. Physical-chemical nature of the aqueous lipids in intestinal content after a fatty meal: revision of the Hofmann-Borgström hypothesis. *Clin. Res.* **28:** 511A.
7. Stafford, R. J., J. M. Donovan, G. B. Benedek, and M. C. Carey. 1981. Physical-chemical characteristics of aqueous duodenal content after a fatty meal. Gastroenterology. **80:** 1291A.
8. Müller, K. 1981. Structural dimorphism of bile salt/lecithin mixed micelles. A possible regulatory mechanism for cholesterol solubility in bile? X-ray structure analysis. *Biochemistry.* **20:** 404–414.
9. Mazur, N. A., G. B. Benedek, and M. C. Carey. 1980. Quasielastic light-scattering studies of aqueous biliary lipid systems. Mixed micelle formation in bile salt–lecithin solutions. *Biochemistry.* **19:** 601–615.
10. Takahasui, Y., and Mizunuma, T. 1984. Cytochemistry of fat absorption. *Int. Rev. Cytol.* **89:** 115–136.
11. Rubin, C. E. 1966. Electron microscopic studies of triglyceride absorption in man. *Gastroenterology.* **50:** 65–77.
12. Jersild, R. A., Jr. 1966. A time sequence of fat absorption in rat jejunum. *Am. J. Anat.* **18:** 135–162.
13. Strauss, E. W. 1966. Electron microscopic study of intestinal fat absorption in vitro from mixed micelles containing linolenic acid, monoolein, and bile salt. *J. Lipid Res.* **7:** 307–323.
14. Marenus, K. D., and F. S. Sjöstrand. 1982. Sequence of structural changes in columnar epithelium of small intestine during early stages of fat absorption. *J. Ultrastruct. Res.* **79:** 92–109.
15. Marenus, K. D., and F. S. Sjöstrand. 1982. The effects of different concentrations of administered fat on the structure of columnar cells in the small intestine. *J. Ultrastruct. Res.* **79:** 110–120.
16. Cardell, R. R., Jr., S. Badenhausen, and K. R. Porter. 1967. Intestinal triglyceride absorption in the rat. *J. Cell Biol.* **34:** 123–155.
17. Howell, J. I., J. A. Lucy, R. C. Pirola, and I. A. D. Bouchier. 1970. Macromolecular assemblies of lipid in bile. *Biochim. Biophys. Acta.* **210:** 1–6.
18. Oh, S. Y., and R. T. Holbach. 1976. Transmission electron microscopy of biliary mixed lipid micelles. *Biochim. Biophys. Acta.* **441:** 498–505.
19. Fromherz, P., and D. Ruppel. 1985. Lipid vesicle formation: the transition from open disks to closed shells. *FEBS.* **179:** 155–159.
20. Weibull, C., A. Christiansson, and E. Carlemalm. 1983. Extraction of membrane lipids during fixation, dehydration and embedding of *Acholeplasma laidlawii*-cells for electron microscopy. *J. Microsc.* **129(2):** 201–207.
21. Dermer, G. B. 1962. An autoradiographic and biochemical study of oleic acid absorption by intestinal slices including determinations of lipid loss during preparation for electron microscopy. *J. Ultrastruct. Res.* **22:** 312–325.
22. Costello, M. J., R. Fetter, and M. Hochli. 1982. Simple procedures for evaluating the cryofixation of biological samples. *J. Microsc.* **125:** 125–136.
23. Phillips, A. M., Jr. 1969. *In* Nutrition, Digestion, Energy Utilization. Fish Physiology. Volume 1. W. S. Hoar and D. J. Randal, editors. Academic Press, New York. 391–432.
24. Dawes, B. 1930. The absorption of fat and lipoids in the plaice. *J. Mar. Biol. Assoc. U.K.* **17:** 75–102.
25. Bauermeister, A. F. M., B. J. S. Pirie, and J. R. Sargent. 1979. An electron microscopic study of lipid absorption in the pyloric caeca of rainbow trout (*Salmo gairdnerii*) fed wax ester-rich zooplankton. *Cell Tissue Res.* **200:** 475.
26. Honkanen, R. E., M. W. Rigler, and J. S. Patton. 1985. Dietary fat assimilation and bile salt absorption in the killifish. *Am. J. Physiol.* **249:** G399–416.
27. Verger, R., G. H. de Hass, L. Sarda, and P. Desnuelle. 1969. Purification from porcine pancreas of two molecular species with lipase activity. *Biochim. Biophys. Acta.* **188:** 272–282.
28. Rovery, M., M. Boudouard and J. Bianchietta. 1978. An improved large scale procedure for the purification of por-

cine pancreatic lipase. *Biochim. Biophys. Acta.* **525:** 373–379.
29. Erlanson, C., P. Fernlund, and B. Borgström. 1973. Purification and characterization of two proteins with colipase activity from porcine pancreas. *Biochim. Biophys. Acta.* **310:** 437–445.
30. Rigler, M. W., R. L. Leffert, and J. S. Patton. 1983. Rapid quantification on Chromarods of cholesterol, total bile salts and phospholipid from the same microliter sample of human gallbladder bile. *J. Chromatogr.* **277:** 321–327.
31. Rigler, M. W., and J. S. Patton. 1984. A simple inexpensive cryogenic storage device for microscopy specimens. *J. Microsc.* **134:** 335–336.
32. Bailey, N. T. J. 1981. Statistical Methods in Biology. John Wiley & Sons, New York.
33. Foster, R., and S. Hong. 1958. In vitro transport of dyes by isolated renal tubules of the flounder as disclosed by direct visualization. Intracellular accumulation and transcellular movement. *J. Cellular Comp. Physiol.* **51:** 259–272.
34. Carey, M. C., and D. M. Small. 1969. Micellar properties of dihydroxy and trihydroxy bile salts. Effects of counterion and temperature. *J. Colloid Interface Sci.* **31:** 382–396.
35. Small, D. M. 1967. Physiochemical studies of cholesterol gallstone formation. *Gastroenterology.* **52:** 607–610.
36. Larsson, K., K. Gabrielsson, and B. Lundberg. 1978. Phase behavior of some aqueous systems involving monoglycerides, cholesterol and bile acids. *J. Sci. Food Agric.* **29:** 909–914.
37. Larsson, K. 1983. Two cubic phases in monoolein–water systems. *Nature.* **304:** 664.
38. Longley, W., and T. J. McIntosh. 1983. A bicontinuous tetrahedral structure in a liquid-crystalline lipid. *Nature.* **303:** 612–614.
39. Hui, S. W., and L. T. Boni. 1982. Lipidic particles and cubic phase lipids. *Nature.* **296:** 175.
40. Deamer, D. W., R. Leonard, A. Tardieu, and D. Branton. 1970. Lamellar and hexagonal lipid phases visualized by freeze-etching. *Biochim. Biophys. Acta.* **219:** 47–60.
41. Eins, S. 1970. Electron microscopy of mesomorphic structures of aqueous lipid phases. I. The system potassium oleate/water. *Mol. Cryst. Liq. Cryst.* **11:** 119–132.
42. Windreich, S., and A. Silberberg. 1980. Interaction of lipid multilayers with water. *J. Colloid Interface Sci.* **77:** 427–433.
43. Gulik-Krzywicki, T., and K. Larsson. 1984. An electron microscopy study of the L-2 phase (microemulsion) in a ternary system: triglyceride/monoglyceride/water. *Chem. Phys. Lipids.* **35:** 127–132.
44. Lindström, M., H. Ljusberg-Wahren, K. Larsson, and B. Borgström. 1981. Aqueous lipid phases of relevance to intestinal fat digestion and absorption. *Lipids.* **16:** 749–754.
45. Carey, M. C. 1982. Measurement of physical-chemical properties of bile salt solutions. *In* Bile Acids in Gastroenterology. L. Barbara, R. H. Dowling, A. F. Hofmann, and E. Roda, editors. MTP Press, Boston, MA. 19–56.
46. Carey, M. C., D. M. Small, and C. M. Bliss. 1983. Lipid digestion and absorption. *Annu. Rev. Physiol.* **45:** 651–677.
47. Knieb, R. T., and A. E. Stiven. 1978. Growth, reproduction and feeding of *Fundulus heteroclitus* on a North Carolina salt marsh. *J. Exp. Mar. Biol. Ecol.* **31:** 121–140.
48. Weisberg, S. B., and V. A. Lotrich. 1982. Ingestion, egestion, excretion, growth and conversion for the mummichog, *Fundulus heteroclitus*. *J. Exp. Mar. Biol. Ecol.* **62:** 237–249.
49. Patton, J. S., R. D. Vetter, M. Hamosh, B. Borgström, M. Lindström, and M. C. Carey. 1985. The light microscopy of triglyceride digestion. *Food Microstruct.* **4:** 29–41.